RSC Advances

ROYAL SOCIETY OF CHEMISTRY

www.rsc.org/advances

Synthesis of Highly Stable and High Water Retentive Functionalized Biopolymer-Graphene Oxide Modified Cation Exchange Membranes

Prem P. Sharma[a,b], Vaibhav Kulshrestha[a,b]*

[a]*CSIR-Central Salt and Marine Chemicals Research Institute (CSIR-CSMCRI),*
Council of Scientific & Industrial Research (CSIR),Gijubhai Badheka Marg,
Bhavnagar- 364 002, (Gujarat), INDIA
Fax: +91-0278-2566970.
E-mail: vaibhavk@csmcri.org, vaihavphy@gmail.com, Tel.: +91-2782567039. Fax: +91278-2567562.

[b] *Academy of Scientific and Innovative Research,*
CSIR-Central Salt and Marine Chemicals Research Institute (CSIR-CSMCRI),
Council of Scientific & Industrial Research (CSIR), Gijubhai Badheka Marg,
Bhavnagar- 364 002, (Gujarat), INDIA

Utility of Polymer electrolyte membrane in energy based devices is substituting the conventional electrolyte. Herein, we have synthesized PEM based biopolymer, functionalized silica modified GO and PVA. GO is modified in two steps to synthesize silica grafted sulfonated GO. Functionalization of chitosan is done using 1,3 propane sultone after deacetylation. Further, PVA has been used as a polymer matrix since PVA possess good film forming property with mechanical stability. Different weight % (1, 2 and 5) of modified GO has been incorporated in the chitosan matrix. Prepared PEMs are subjected to different characterization such as structural, thermal, mechanical and electrochemical etc. The nano-hybrid membranes shows the significant increment in electrochemical properties. MGO-SCH-5 membrane shows the proton conductivity as 6.77 $\times 10^{-2}$ S cm^{-1} which goes to increases upto 11.2×10^{-2} S cm^{-1} at 90^0C. Thermal and mechanical stability of PEM also gets increases with the MGO content in to sulfonated chitosan. The elastic modulus for MGO-SCH-5 membrane is calculated to 21.37 MPa with 54 MPa of maximum stress. Thus membranes may be targeted as PEM for higher temperature energy application.

Key words: Chitosan; Functionalized Graphene oxide; Ionic conductivity; Thermo-mechanical properties.

Introduction

Polymer electrolyte membranes (PEM) are playing a vital role in energy based devices, and replacing liquid electrolyte in fuel cells and batteries due to their ease of handling and excellent physico-chemical as well as mechanical properties etc. [1-4]. Composite membranes are the subject of intense research as well as are ideal work of art due to its excellent properties [5-6]. To date, various kind of fillers have been incorporated into polymer matrix to enhance the membrane performance for different applications [7-10]. Different type carbon based materials such as carbon quantum dots, graphene oxide, C 60 and carbon nanotube have been incorporated within the polymeric membranes and they have displayed significant enhancement in the membrane performance. Different types of oxides and conducting polymers have also been incorporated into the PEM to enhance its applicability and stability [11-12]. An ideal PEM must have high ionic conductivity, high thermal, mechanical stability and high methanol crossover resistance to be employed as solid electrolyte for fuel cell application. Fascinating properties of Graphene oxide (GO) makes it a material of interest and in past few years research on GO is rising and it can be estimated by the increasing number of publications [6]. Applicability of GO has been realized for many applications and many other are yet to be explored [13]. Use of GO in polymer electrolyte membrane has been done in our previous work [7]. Further, GO has also been modified with different metals, metal oxides etc. by many researchers [8]. Modification of GO with silica is an effective strategy to increase the stability of material, since silica is a low cost and abundant material. GO-silica composite has been prepared by Zhang et. Al. for electroreponsive characteristics [9]. High ionic conductivity is a basic requirement for PEM and sulfonation is an effective way of increasing the proton conducting groups in the membrane. Sulfonation of GO enhances the ionic conductivity as well as its applicability for different applications. Hu et. al. studied the Proton transport through monolayer graphene and hexagonal boron nitride (hBN) and observed that monolayers of graphene and hBN constitute a class of proton conductors with high proton conductivity, chemical and thermal stability, and resistive to H_2, water and methanol make these membranes attractive candidates for use in various hydrogen technologies. [10]. Chitosan is a natural polymer obtained from chitin and used as a membranes for many applications such as water desalination, batteries etc. [11]. Sulfonation of chitosan enhanced its proton conductivity due to the addition of sulfonic acid groups. Poly vinyl alcohol (PVA) is a water soluble polymer and have good film forming property, used as the plasticiser for membrane applications [12-15]. Interaction between PVA and GO is due to the hydrogen bonds that may remarkably improve its properties. The main drawback of PVA is that it dissolves in water, to overcome this problem PVA can be cross-linked with formaldehyde.

We report the synthesis and electrochemical properties of silica modified sulfonated GO and sulfonated chitosan based PVA membrane as polymer electrolyte membranes. Different concentration of modified GO has been incorporated within the chitosan matrix to prepare its membrane. Hybrid membranes shows the better electrochemical properties with higher stability and may prove a good candidate for PEM.

Experimental

Materials and methods

Chitosan with medium molecular weight, (3-Aminopropyl) triethoxysilane (APTEOS), N, N'-Dicyclohexylcarbodiimide (DCC) and Graphite is purchased from Sigma Aldrich. Acetic acid with average molecular weight ~ 60.05 and density ~ 1.048-1.050 g/ml was purchased from Fischer Scientific. 1, 3-Propane sultone with average molecular weight ~ 122.14 was purchased from TCI. Whole reaction was carried out in deionized water. All other chemicals were obtained commercially and used as received without further purification.

Synthesis of Graphene Oxide (GO) and modified Graphene Oxide (MGO)

The preparation of graphene oxide from graphite powder was done by modified Hummer's method reported earlier [16, 17]. Now conversion of GO into MGO is done in two step process. Firstly, the reaction of graphene oxide was carried out with (3-Aminopropyl) triethoxysilane then sulfonation of APTEOS modified GO is carried out using concentrated sulfuric acid followed by chlorosulfonic acid. Briefly, 100 mg of graphene oxide and 5 mg DCC is added to 10ml APTEOS followed by sonication of 60 minutes. After that the whole mixture is transferred into a 100 ml round bottom flask and refluxed at 70°C with continuous stirring for 24 hrs under nitrogen atmosphere. Then the mixture is allowed to cooled and precipitated in absolute ethanol [18]. The solution is centrifuged severally. Finally the product is dried at 60°C in vacuum for whole night. Further, APTEOS modified GO is sulfonated using concentrated sulfuric acid followed by chlorosulfonic acid [17]. Briefly, 100 mg of APTEOS modified GO is treated with 75 ml concentrated sulfuric acid at least for 1 hour and then addition of 15 ml chlorosulfonic acid is done drop wise. The whole reaction was stirred at room temperature for 24 hrs. Afterwards, the solution is slowly added in diethyl ether at 0-5°C. The whole reaction mixture is then centrifuged at 6000 rpm to get the desired product. The product was then dried under vacuum at 60°C for overnight. This product is designated as MGO as shown in Scheme 1.

Synthesis of sulfonated chitosan and their membranes

The chemical reaction of deacetylated chitosan with that of the 1,3 propane sultone is carried out to obtain pendent sulfonated chitosan. The resultant product will be the chitosan-N-propyl sulfonic acid [19]. Briefly, 1gm of chitosan was mixed into 80 ml of 2 wt% of acetic acid and the reaction mixture is stirred at room temperature for 1-2 hours to get a homogeneous mixture. Now 0.4 g of 1,3- Propane sultone was added drop wise and the mixture is allowed to stirrer at 65-70° C for 6 hours. After achieving the room temperature the reaction mixture is poured in acetone. The product is chitosan-N-propyl sulfonic acid. Now the product dried under vacuum at room temperature and is designated as SCH as shown in Scheme 1. FTIR spectrum of sulfonated chitosan Fig. S1.

The MGO-SCH based hybrid membranes are obtained by getting a homogeneous mixture of sulfonated chitosan and MGO in deionized water. As graphene oxide has abundant oxygen in form of –OH (hydroxyl), -COOH (carboxyl), and epoxy ring functional groups which make GO more hydrophilic and also its dispersion in deionized water is stable. Briefly, 3g of sulfonated chitosan is mixed with deionized water at room temperature. In addition to it 3g of poly (vinyl alcohol) is again mixed with the deionized water. Afterwards add both the reaction mixtures and wait until the mixture becomes homogeneous. Membranes with different MGO concentration (1%, 2% and 5%) with sulfonated chitosan are prepared successfully and designated as MGO-SCH-1, MGO-SCH-2 and MGO-SCH-5 respectively. Briefly desired amount of MGO is added to the homogeneous mixture of Poly (vinyl alcohol) and sulfonated chitosan in deionized water. Now this reaction mixture is subjected to continuous stirring until we get a stable dispersion of MGO particle within the matrix. Afterwards this solution is casted on a clean glass plate. Dry it at 80° C for overnight and peel off with the help of sharp blade. Now the resultant dried film is further subjected to cross linking with formaldehyde to convert it into water insoluble. In a typical crosslinking reaction the films are immersed in a solution containing formaldehyde (55.0 g), sodium sulfate (150.0 g), sulfuric acid (125.0 g) and water (470.0 g) for 3 h at 60°C.

Chemical and Structural Characterization of Hybrid Membrane

The study of chemical and structural characterization of the materials and membrane was done by using ^{1}H NMR, FTIR, XRD, TEM and AFM. The fourier transform infrared spectra (FTIR) spectra of MGO and MGO-SCH hybrid were recorded at a frequency 4000-400 cm^{-1} using KBR pellets with the help of spectrum GX series 49387 spectrometer. X-Ray Diffraction of GO, MGO and MGO/SCH membrane was carried out by using Philip's X'Pert MPD system by using CuKα radiation with a scattering range of 5 to 60°. Transmission Electron Microscopy was carried out by using JEOL, JEM 2100 microscope with an accelerating voltage of 200 keV. The surface roughness was recorded by using Atomic Force Microscopy (AFM) in semi contact mode on NTEGRA AURA (NTMDT).

Thermal and Mechanical Stabilities of Hybrid Membrane

Thermal behavior of MGO and MGO-SCH in terms of the degradation and stability were measured with the help of thermo-gravimetric analyzer (TGA) under N_2 atmosphere on Mettler Toledo TGA/SDTA851e with stare software, with a heating rate of 5 °C/min from 25 to 600°C. The glass transition behavior of hybrid membranes was assessed through differential scanning calorimetry (DSC) using Mettler Toledo DSC822e thermal analyzer under temperature range 0 to 200°C. Universal Testing Machine (UTM) was used to assess the mechanical properties of hybrid membranes under room temperature.

Physiochemical and Electrochemical Characterization of Hybrid Membrane:

Water Uptake behaviour of membranes was determined by recording the weight gain after equilibrating in water for 24h. Ion exchange capacity of hybrid membranes was estimated by the acid base titration. Proton conductivity of the membranes was measured on potentiostat/galvanostat (Auto Lab, Model PGSTAT 30). Proton diffusion coefficient for the membranes is calculated using membranes conductivity measurements. Details of the experiments are given in ESI.

Methanol crossover resistance:

Methanol permeability for the membranes are evaluated by the measurement with two compartment cell. Details of the experiment and formula used are described in Electronic Supplementary Information (ESI) section.

Results and discussion

Chemical and Structural Characterization of MGO and Hybrid Membranes:

The interaction between SCH and MGO is shown in Scheme 1. It is clear from the scheme that SCH is attached with MGO with hydrogen bonding. FTIR spectra of MGO, SCH and hybrids of MGO and SCH are presented in Fig. 1. IR spectra of prepared materials and hybrids show a broad peak at 3420-3434 cm^{-1} which is due to the existence of large number of hydroxyl and amino groups. The bands near to 1622 cm^{-1} are due to the presence of the stretching of acetyl groups present in chitosan. The detection of sulfonic acid hydrates absorption bands are nearly from 2400-2000 cm^{-1} and the characteristic peaks of –OH, -SO_3H and amide groups are at 3434, 2918, 1625 cm^{-1} respectively [20]. IR peaks in the region of 1552 and 1535 cm^{-1} indicates the presence of sulfonation reaction occur in the amino group present in the chitosan. The peak at 1115cm^{-1} in MGO demonstrates the presence of –SO_3H functional group [17, 21]. The appearance of a narrow peak nearby to 1051 cm^{-1}(Si-O-C/Si-O-Si) demonstrates the evidence of successful chemical functionalization of graphene sheets [22]. Moreover, the FTIR results clearly say about the formation of MGO and MGO-SCH nano-hybrid membrane. ^1H NMR spectrum of sulfonated chitosan hybrid membrane are shown in Fig. S2. ^1H NMR predicts us about the substitution of the chitosan. Enhanced chemical shift values at 3.41 and minor peak at 3.18 states about the reduction of the free amino groups [23]. This decrease in the free amine group indicated about the substitution takes place on free primary amine. The diffused peaks nearby to 2.3 ppm is due the overlapping of the signals comes out from the overlapping of –OH and –NH groups in form of –CH_2N. The structural analysis of GO, MGO and MGO-SCH hybrid membranes are shown in Fig. 2. GO has a diffraction angle and inter-planer spacing values at 11.16° and 7.92Å. On the other hand in case of MGO there are found two values of the diffraction angle secondly at 22.41°and a shifting in the value of diffraction angle which is greater than previous and comes out to be 11.92° which is a result of the partial rearrangement through $\pi-\pi$ interaction and the removal of oxygen functional groups and also due to the inserting of the sulfonic acid group within the GO [24]. The interaction of the MGO with that of the biopolymer can be seen in the figure where the value of the diffraction peak comes out to be 19.44°. Fig. 3 shows the TEM images of GO and MGO at different magnifications. Sheet like structure of GO can be seen in Fig. 3(A), while Fig. 3(B) shows the micrograph of modified GO. Uniformly distributed Si nanoparticle of 4nm can be seen throughout the GO matrix. Fig. 3(C) shows the MGO at higher magnifications. Average roughness of the SCH and MGO-SCH hybrid membranes is calculated using AFM imaging. The average roughness of the membranes are found to be 4.254 nm in case of the SCH membrane which goes to increase by 7.835 nm for MGO-SCH hybrid membrane. The respective AFM images are shown in the Fig. 4. The transparency of the hybrid membrane goes to decrease by adding the MGO amount into the SCH and can be seen in Fig. 9.

Stability of MGO and Hybrid Membranes:

Thermal stability of the MGO and membranes are presented in Fig. 5. Fig. 5 (A) shows the TGA and DTG thermograph of MGO. Two step weight loss is observed from the spectrum one is due to the degradation of sulfonic acid group and second is due to the degradation of Si. Thermal degradation study of the chitosan and MGO-SCH based nano-hybrid membranes are presented in Fig. 5(B). Thermal studies show three stages of decomposition. First, loss in the weight was measured due to the vaporization of the moisture content; second stage weight loss was due to the breakdown of bond established due to the functional groups that may be volatile also. Third stage breakdown is due to the disintegration of the polymer backbone. The loss at first stage comes nearly to be 11% in a range between 80-200°C and the second stage follows a weight loss of about 25%in the range just above 250°C which is due to the pendent sulfonic acid groups present in the chitosan similarly the third stage weight loss 75% will be found in a region nearly about 450-550°C is due to the breaking of the chitosan skeleton [24]. DSC thermogram of SCH and MGO-CHT based hybrid membrane are shown in Fig. 6. It can be seen from the figure that T_g of hybrid membranes increases with MGO content into the matrix and MGO-SCH-5 membrane shows the higher thermal stability compared to other membranes, which is also verified by TGA analysis [25].

The well dispersion of MGO within the polymer matrix expects a good augmentation. To get a desired result tensile test is performed for all the polymer electrolyte nano-hybrid membranes. A typical stress-strain curve is obtained and there mechanical properties were compared as shown in Fig. 7. It can be seen in the figure that the incorporation of MGO within the polymer matrix in MGO-SCH-5 makes the polymer-electrolyte membrane more mechanically stiff and stable as compared to SCH membrane. The values of the elastic modulus increases in an interesting manner from SCH to MGO-SCH-5 as 8.66 MPa to 21.37 MPa respectively Table [1]. On the other hand maximum stress of the hybrid membranes also increasing from 21.64 MPa to 54 MPa. We can conclude that as the concentration of MGO increases from 1% to 5% the stiffness of the membrane will also be superior respectively. Hence, the elongation of the hybrids with higher concentration will found to be lesser than SCH. The maximum elongation at break (strain %) 19.61 is found for SCH which goes to decreases by 68% and reached to 6.2 in MGO-SCH-5 membrane Table [1]. The interfacial interaction of the MGO with the polymer matrix restricts the polymer chain movement as in result leading the membrane too brittle. Thus, this consistency of result helps us to predict the very well interaction of the filler with that of the polymer matrix and that contributes the empowerment of the mechanical strength of the polymeric electrolyte membrane.

Water Uptake Behaviour, Water Retention Capability and Ion exchange capacity (IEC) of Hybrid Membranes:

Water retention capability and water uptake are play a very important role to make a PEM's and its further application for energy devices. Water uptake as observed in the prepared membrane show an increasing trend from SCH to MGO-SCH-5. SCH membrane displays 27% water uptake and goes to increases by increasing the MGO content. 43% of water uptake is observed in MGO-SCH-5 membrane (Table 2). Higher water uptake in membrane leads to higher proton conduction in PEM. Bound water and free water values are also obtained from TGA curves. It is evident from Table 2 that bound water is increasing as the MGO content increases. SCH membrane contains the 0.45 % bound water which increases up to 0.96% after addition of 5 wt% MGO to the membrane. Furthermore, the calculated free water is also found to be highest in MGO-SCH-5 membrane i.e. 42.04%. Bound and free these two kinds of water are present in a membrane. Bound water is more responsible for the proton conduction in PEM at higher temperature. Higher water uptake leads the dimensional instability in PEM, but in present case dimensional stability increases with water uptake this may be due to the interaction between SCH and MGO [5,6].

IEC is the key parameter for the performance of proton exchange membrane (PEM) which mainly depends upon the degree of functionalization of the polymer. Higher functional group leads to the higher IEC in PEM. SCH membrane shows the 1.56 meq/gm IEC value which goes to increase 2.08 meq/gm for MGO-SCH-1 membrane and finally attained to 2.56 meq/gm for MGO-SCH-5 membrane, the value for MGO-SCH-5 is 25% higher that of SCH membrane (Table 2). Thus it can be seen that the IEC values gradually increases as increases the MGO loading within the membrane matrix. It is due to the free carboxylic group present within the polymer matrix. The sulfonic acid group channels inside the polymer matrix and interfacial interaction in between the –COOH group of the MGO and $–SO_3H$ group of the sulfonated chitosan make the whole hybrid more hydrophilic thus provides a capacity in favours the counter ion to pass through it and thus a gradually increase in the capacity to exchange the ions.

Effect of Temperature on Ionic conductivity of Hybrid Membranes:

Membrane proton conductivity is measured for all hybrid membrane from 30 to 90°C and the corresponding values are illustrated in Fig. 8 & Table 2. The proton conductivity increases with MGO content in membranes due to enhanced proton mobility resulting from the increased water retention capability. The proton conductivity of the SCH membrane is calculated to 3.28×10^{-2} S cm^{-1} at 30°C, which raised up to 6.77×10^{-2} S cm^{-1} for the MGO-SCH-5 membrane. Comparison of ionic conductivity with reported membranes are presented in Table 3. The increment in conductivity is due to the higher IEC, higher water retention capacity and higher number of available sulfonic group sites in the membrane. High IEC provide more acidic groups inside the membrane and a presence of high bound water makes the proton diffusion easy [26, 29]. Acidic functional groups ($–SO_3H$) of PEM dissociate due to hydration and allow transport of hydrated proton $(H_3O)^+$. For higher temperature applications the membranes are tested for their conductivity from 30 to 90°C and found that temperature can moderate the conduction of proton. As the temperature increases the migration of ions gets fast resultant increment in conductivity of hybrid membrane. The membranes conductivity found to be increased from 1.55 to 1.63 times for SCH to MGO-SCH-5 membrane on increasing the temperature from 30 to 90°C. The increment in proton conductivity at higher temperature may be due to the increment proton migration [30, 31]. In case of MGO-SCH-5 membrane the conductivity is comparable with Nafion-117 membrane for whole temperature range [32].

Methanol permeation (P_M) of hybrid membranes:

Low methanol permeation with high proton conductivity is the basic requirement for PEM for DMFC application. Methanol permeability of SCH and MGO/SCH hybrid membranes are presented in Table 2. It is clear from the data that methanol permeation resistance of hybrid membrane increases with MGO content in SCH matrix. The methanol permeation resistance of SCH membrane is found to be 2.6 X 10^{-6} cm^2S^{-1}, which reduces to 1.01 X 10^{-6} cm^2S^{-1} for MGO-SCH-5 hybrid membrane, the selectivity of the membrane is found to be enhanced by 5.3 times to its initial value 1.26 x10^4 for SCH membrane. The low methanol permeability and high selectivity of MGO-SCH-5 membrane makes it applicability for DMFC.

Conclusion:

In summary, we designed a biopolymer PEM having superior performance based on sulfonated chitosan as a functionalized biopolymer and modified graphene oxide with stable thermal and mechanical property. The properties of the membranes are summarized is Fig. 9. The modified graphene oxide shows an extensive interfacial interaction with sulfonic acid group of the biopolymer resulting the formation of strong chemical bonding which in results provide good mechanical strength and stiffness to the PEM. MGO-SCH-5 membrane shows good value of modulus 21.37 MPa with 54 MPa of maximum stress and good ion-exchange capacity which is 2.56 meq/gm. MGO-SCH-5 membrane shows the stability at higher temperature upto 300 ^{0}C with better electrochemical performance. The proton conductivity of MGO-SCH-5 membrane is calculated to be 6.77 $\times10^{-2}$ S cm^{-1} which goes to increases upto 11.2$\times10^{-2}$ S cm^{-1} at 90^{0}C. The maximum ionic conductivity has been found in MGO-SCH-5 hybrid membrane with higher methanol crossover resistance and selectivity. The synergistic approach can be derived for a candidate in the promising area of energy conservation and for high temperature polymer electrolyte cells. Moreover the materials used to make these membranes are eco-friendly and non-hazardous, economically cheap and naturally abundant.

Acknowledgments

Author V. Kulshrestha is thankful to Department of Science and Technology, New Delhi, for providing fund under WTI scheme. Financial support received from CSIR Network projects no.

CSC 0105 is also acknowledged. Authors are also thankful to Analytical Division and Centralized Instrument facility, CSMCRI, Bhavnagar for instrumental support.

Supporting Information:

The detail of the chemical, structural, physiochemical characterization & membranes stability are included as section S1 in supporting information. Fig. S1 to S2 are also included in supporting information section.

References:

1. Sharma, P.P; Gahlot, S.; Bhil, B.M; Gupta, H.; Kulshrestha, V. *RSC Adv.*, **2015, *5,*** 38712.
2. Lufrano, F.; Baglio, V.; Staiti, P.; Antonucci, V.; Arico, A.S. *J Power Sources*, **2013, *243***, 519.
3. Dutta, K.; Das, S.; Kumar, P.; Kundu**,** P.P. *Appl. Energy*, **2014, *118*,** 183.
4. Xu, K.; Chanthad, C.; Gadinski, M. R.; Hickner, M. A.; Wang, Q. *ACS Appl. Mater. Interfaces*, **2009, *1*,** 2573.
5. Gahlot, S.; Kulshrestha, V. *ACS Appl. Mater. Interfaces*, **2015**, *7***,** 264.
6. Gahlot, S.; Sharma, P.P; Kulshrestha, V.; Jha*,* P. K. . *ACS Appl. Mater. Interfaces* **2014**, *6,* 5595.
7. Gahlot, S.; Sharma, P.P; Gupta, H.; Kulshrestha, V.; Jha*,* P. K. *RSC Adv.*, **2014*, 4,*** 24662
8. Li, X.; Yu, Y.; Meng, Y. *ACS Appl. Mater. Interfaces*, **2013, *5***, 1414.
9. Klaysom, C.; Moon, S. H.; Ladewig, B. P.; Lu, G. Q. M.; Wang, L. Z. *J. Phys. Chem C.*, **2011, *115,*** 15124.
10. Hu, S.; Lozada-Hidalgo, M.; Wang, F. C. ; Mishchenko, A.; Schedin, F.; Nair, R. R.; Hill, E. W.; Boukhvalov, D. W.; Katsnelson, M. I.; Dryfe, R. A. W.; Grigorieva, I. V.; Wu, H. A. ; Geim, A. K.; *Nature* **2014**, ***516***, 227.
11. Perreault, F.; Tousley, M. E.; Elimelech*,* M. *Environ. Sci. Technol. Lett.*, **2014, *1***, 71.
12. Kumar, A.; Gahlot, S.; Kulshrestha, V.; Shahi, V. K. AIP Conference Proceedings **2014, *1591,*** 379.
13. Kumar, M.; McGlade, D.; Lawler J. *RSC Adv.*, **2014*, 4,*** 21699.

14. Sharma, R.; Singh, N.; Gupta, A.; Tiwari, S.; Tiwari, S.K.; Dhakate, S.R. J Mater. Chem. A, **2014,** ***2***, 16669.
15. Palani, P. B.; Abidin, K. S.; Kannan, R.; Sivakumar, M.; Wang, F.M.; Rajashabala S.; Velraj, G. *RSC Adv.*, **2014,** ***4,*** 61781.
16. Chabot, V.; Higgins, D.; Yu, A.; Xiao, X.; Chen, Z.; Zhang, J. *Energy Environ. Sci*. **2014,** *7,* 1564.
17. Yu, D.; Negelli, E.; Naik, R.; Dai, L. *Angew. Chem. Int. Ed.* **2011**, ***50,*** 6575.
18. Yang, H.; Li , F.; Shan , C.; Han, D.; Zhang, Q.; Niu, L.; Ivaska A. *J. Mater. Chem.,* **2009,** ***19,*** 4632.
19. Tsai , H. S.; Wang , Y. Z.; Lin , J. J.; Lien , W. F. *J. Appl. Polym. Sci*., **2010,** ***116,*** 1686.
20. Jeon, J.H.; Cheedarala, R. K.; Kee , C.D.; Oh, I.K. Adv Funct. Mater. **2013,** ***23,*** 6007.
21. Kumar, R.; Scott, K. *Chem. Commun*., **2012,** ***48,*** 5584.
22. Xie, X.; Qu, L.; Zhou, C.; Li, Y.; Zhu, J.; Bai, H.; Shi, G.; Dai, L. *ACS Nano*, **2010**, ***4***, 6050.
23. Sharma, R.; Singh, N.; Tiwari, S.; Tiwari, S.K.; Dhakate, S.R., *RSC Adv.*, **2015,** ***5,*** 16622.
24. Vongchan, P.; Sajomsang, W.; Subyen, D.; Kongtawelert, P.; *Carbohydrate Research* **2002,** ***337,*** 1239.
25. Gahlot, S.; Sharma, P.P; Kulshrestha, V. *Separation Science and Technology,* ***2015, 50,*** *446.*
26. Zarrin, H.; Higgins, D.; Jun, Y.; Chen, Z.; Fowler, M. *J. Phys. Chem. C* **2011**, ***115,*** 20774.
27. Heo, Y.; Im, H.; Kim, J. *J. Membr. Sci.* **2013**, 426, 11.
28. Lin, C.W.; Lu, Y.S. *J. Power Sourc.* **2013**, ***237,*** 187.
29. Choi, B.G.; Hong, J.; Park, Y.C.; Jung, D.H.; Hong, W.H.; Hammond, P.T.; Park, H.S. *ACS Nano* **2011**, ***5,*** 5167.
30. Petrowsky M.; Frech R. *J. Phys. Chem. B* **2010**, ***114,*** 8600.
31. Filipoi C.; Demco D.E.; Zhu X.; Vinokur R.; Conradi R.; Fechete R.; Möller M. *Chem. Phys. Lett.* **2012,** ***554,*** 143.
32. Jiang, Z.; Zhao, X.; Fu, Y.; Manthiram, A. *J. Mater. Chem.* **2012**, ***22,*** 24862.
33. Bhadja, V.; Chatterjee, U.; Jewrajka, S.K. *RSC Adv.,* **2015, 5,** 40026.
34. Tripathi, B.P.; Schieda, M.; Shahi, V.K.; Nunes, S.P. *J. Power Sources*, **2011,** ***196*** 911.

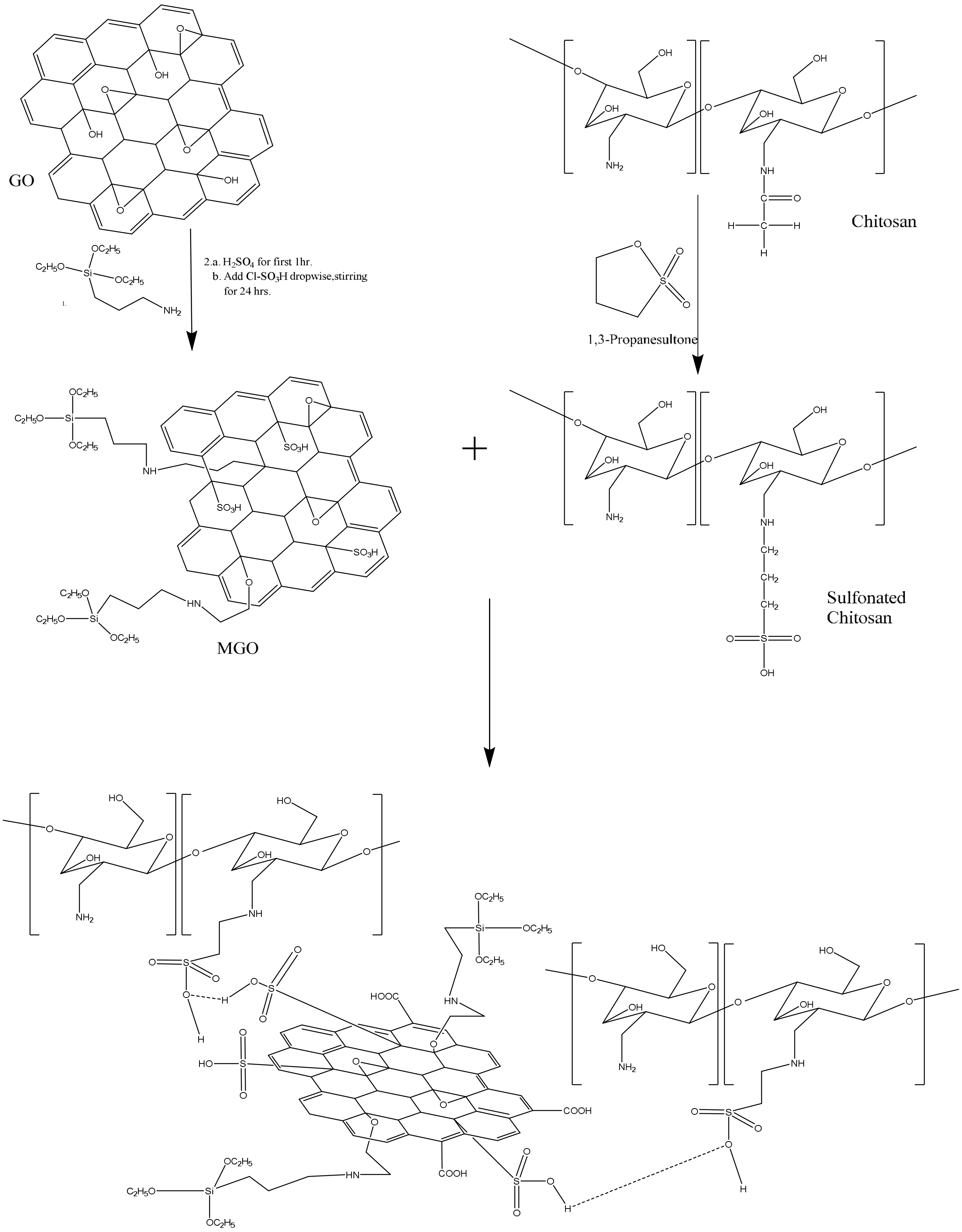

MGO modified Sulfonated Chitosan

Scheme 1: Conversion of Graphene Oxide and Chitosan to modified Graphene Oxide

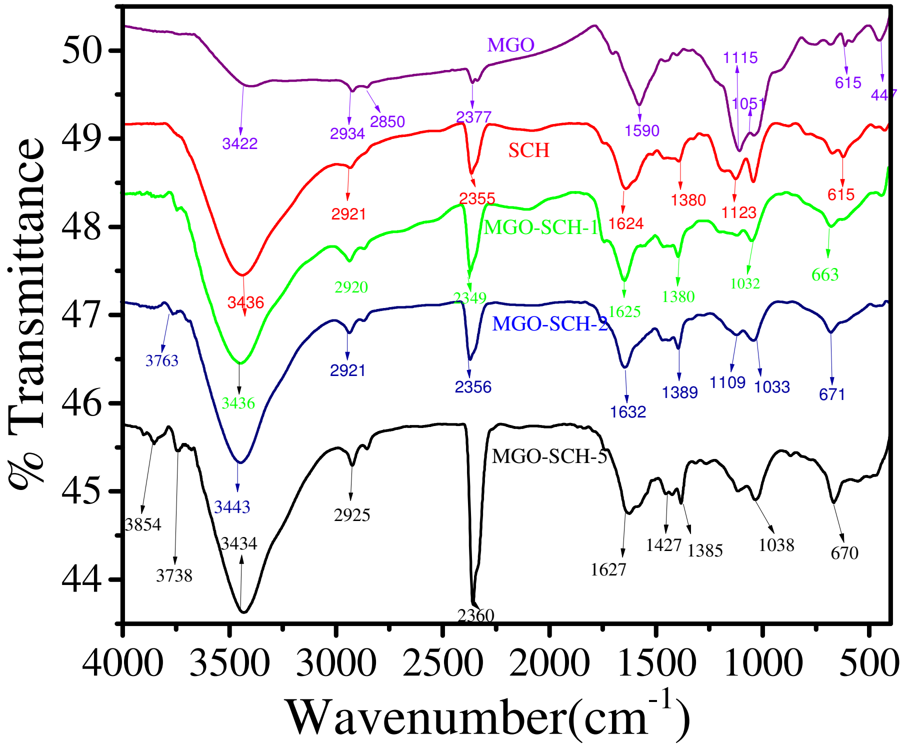

Fig. 1: FTIR spectra of MGO, SCH and their hybrid membranes

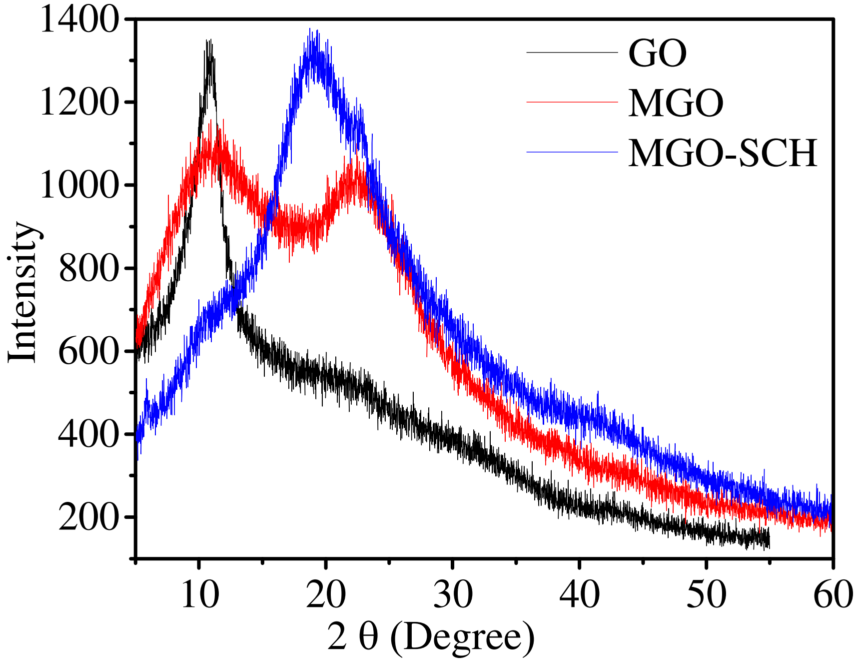

Fig. 2: XRD spectra of GO, MGO and their hybrid membrane

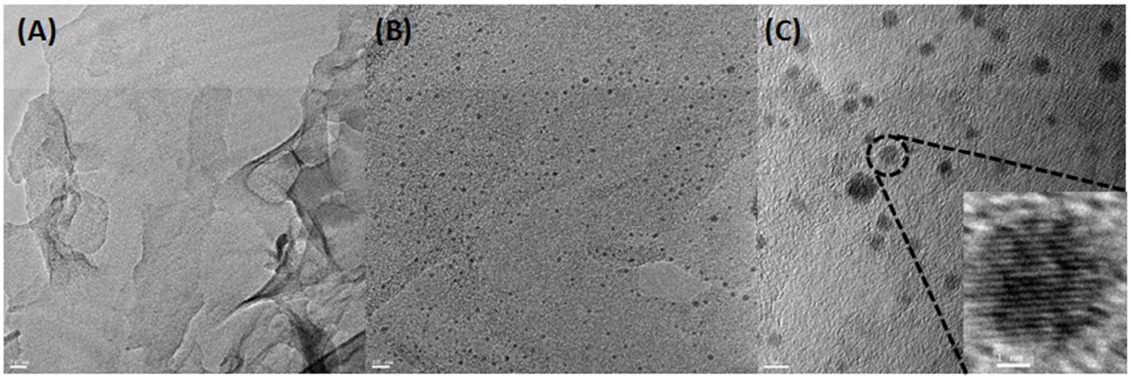

Fig. 3: TEM images of (a) GO (b & c) MGO at different magnifications

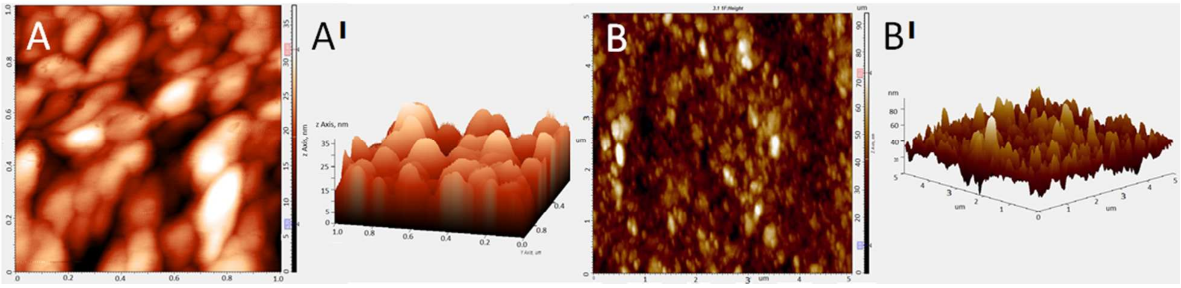

Fig. 4: AFM images of (A, A') SCH and (B, B') MGO-SCH-5 membranes

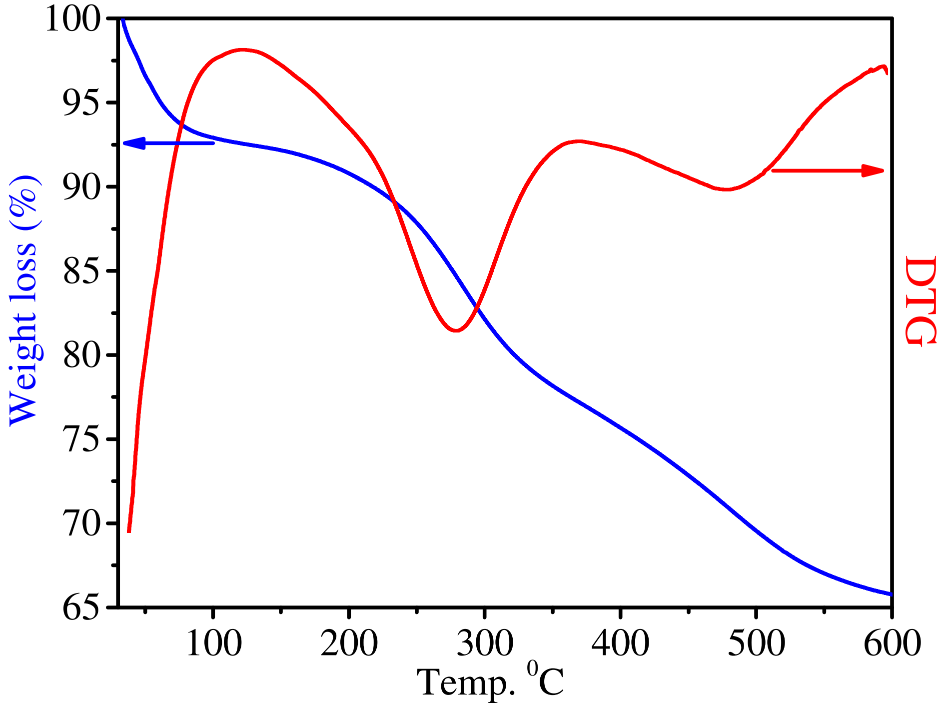

Fig. 5 (A): TGA and DTG thermograph of MGO.

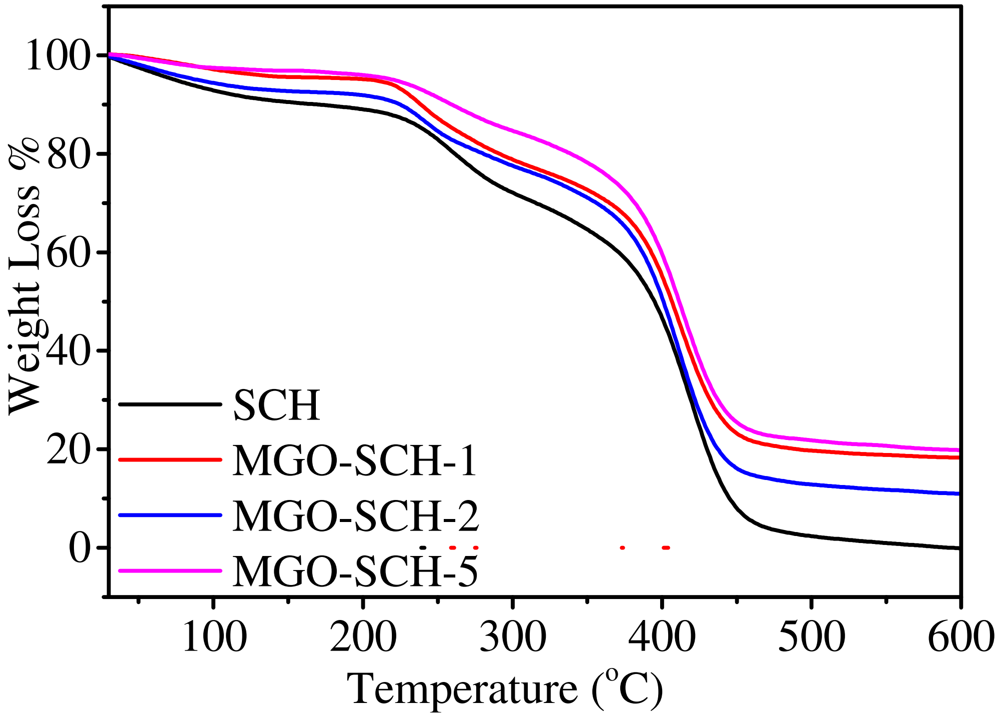

Fig. 5(B): TGA of SCH and MGO-CHT based hybrid membrane.

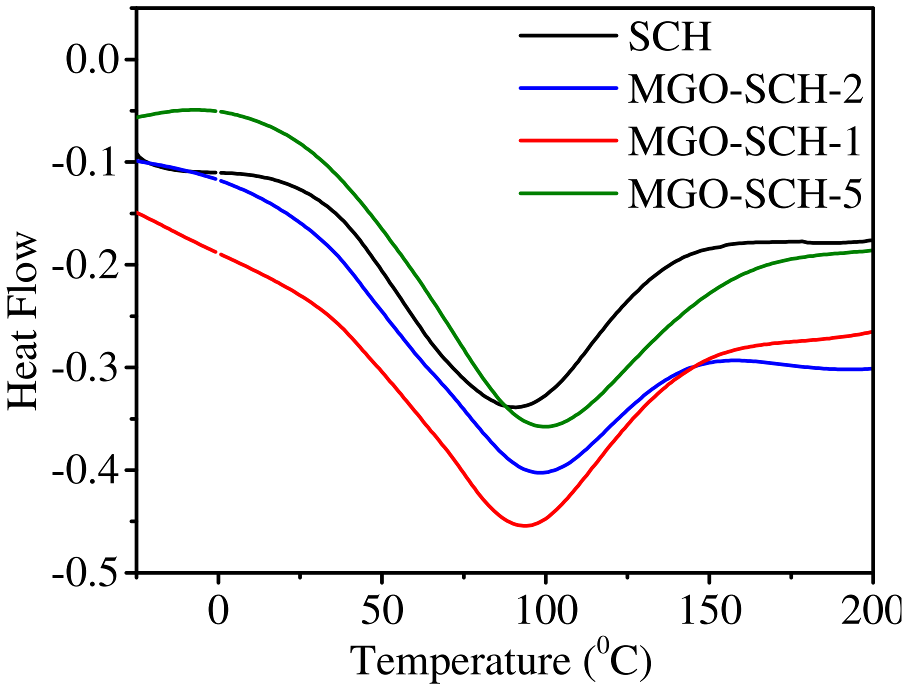

Fig. 6: DSC thermogram of SCH and MGO-CHT based hybrid membrane.

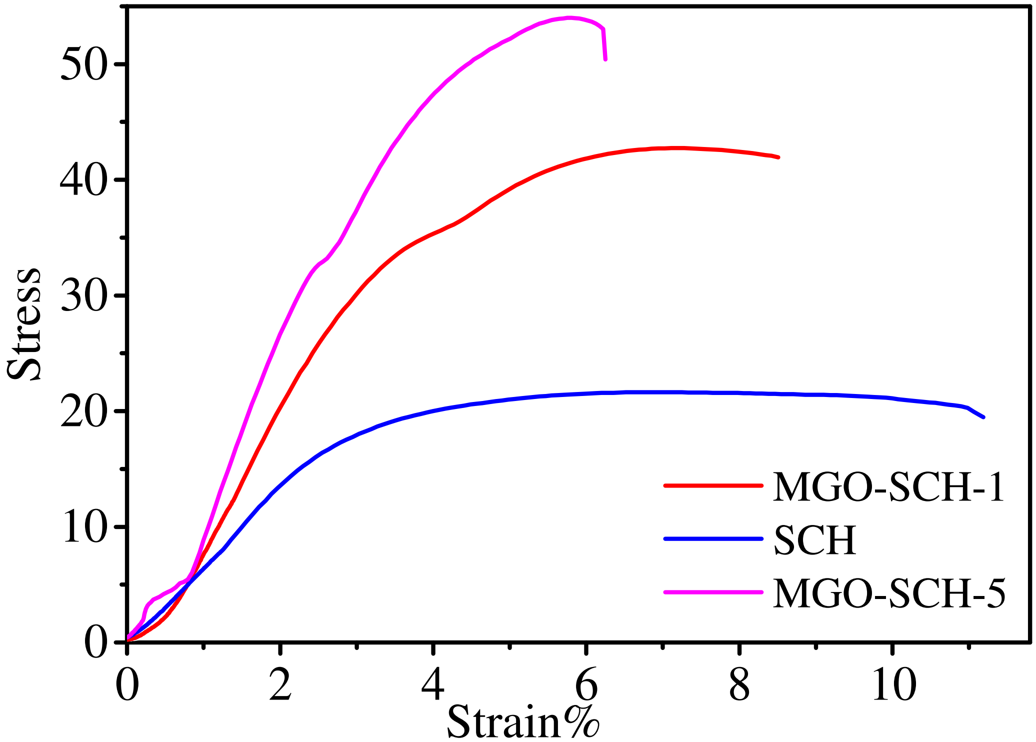

Fig. 7: UTM analysis of SCH and MGO-CHT based hybrid membrane.

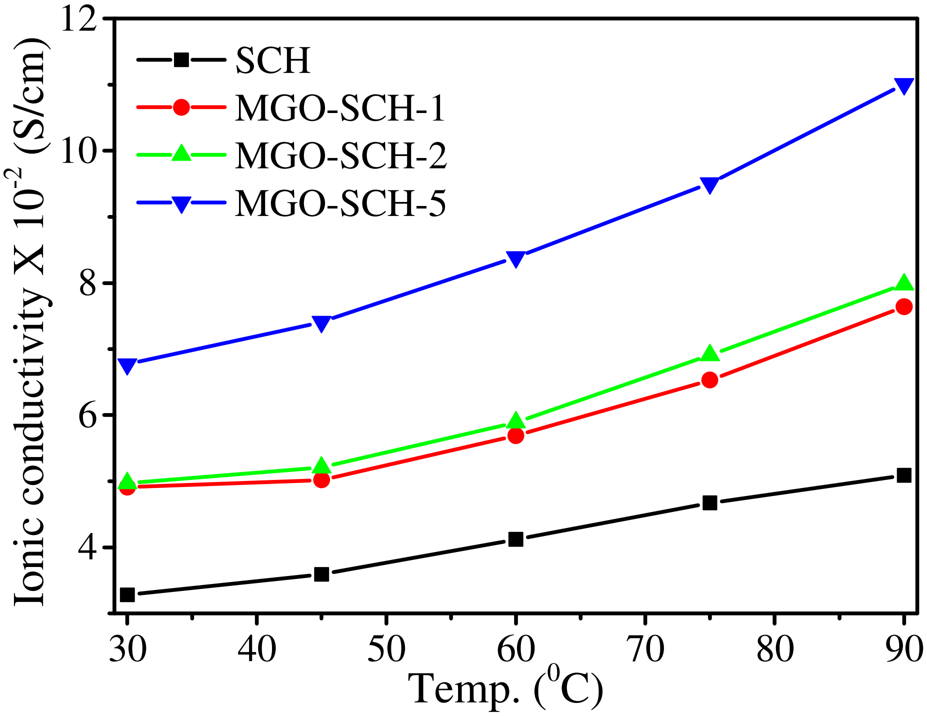

Fig. 8: Temperature versus ionic conductivity for different hybrid membrane.

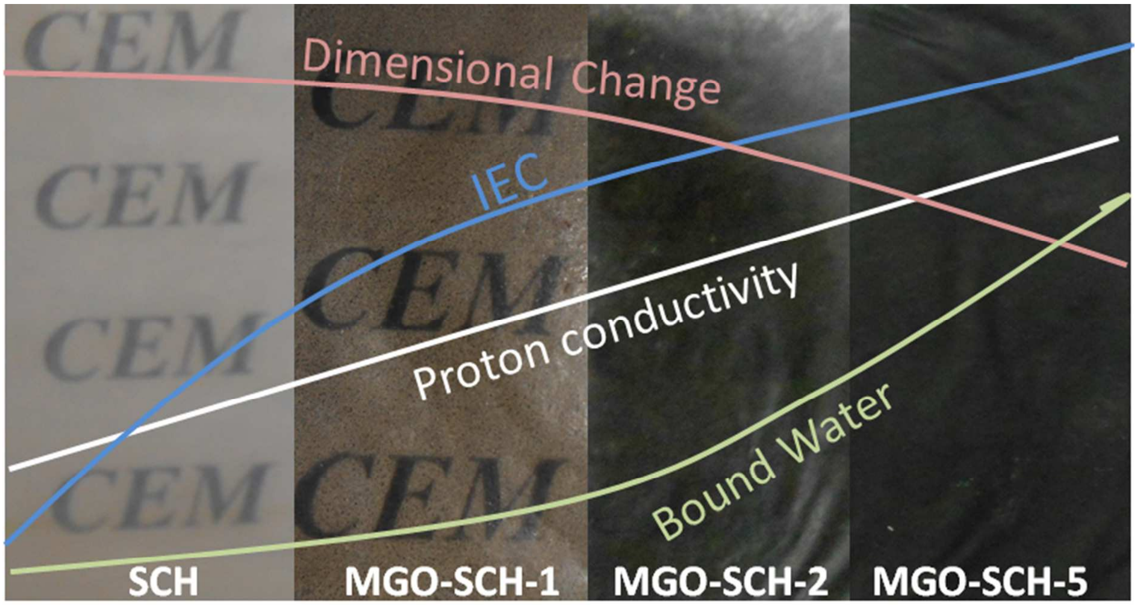

Fig. 9: Different properties for hybrid membrane.

Table 1: Mechanical properties of different membranes

Membrane Type	Young's Modulus (MPa)	Maximum Stress (MPa)	Elongation at break %
SCH	8.66	21.64	19.61
MGO-SCH-1	16.55	42.73	8.5
MGO-SCH-5	21.37	54.0	6.2

Table 2: Ion exchange capacity (IEC), water uptake (W), bound and free water (%), dimensional stability, ionic conductivity (φ), methanol permeability (Pm) and selectivity (Sp) for different membranes.

Membrane Type	IEC (meq/g.)	W (%)	Bound water %	Free Water %	Dimensional Change %	$\varphi \times 10^{-2}$ (S/cm)	$Pm \times 10^{-6}$ (cm^2/s)	$Sp \times 10^4$
SCH	1.56	27	0.45	26.55	38.14	3.28	2.60	1.26
MGO-SCH-1	2.08	30	0.50	29.50	28.57	4.91	1.90	2.58
MGO-SCH-2	2.40	36	0.63	35.37	25.73	4.97	1.60	3.1
MGO-SCH-5	2.56	43	0.96	42.04	24.48	6.77	1.01	6.71

Table 3. Comparison of Ionic conductivity of the present membrane with reported.

Membrane Type	IEC (meq/gm)	Ionic Cond. $\times 10^{-2}$ (S/cm)	Ref.
10 % MWCNT in SPEEK	1.84	4.47	34
CEM-3	1.50	1.37	33
SG-10	1.27	6.40	7
MGO-SCH-5	2.56	6.77	This study

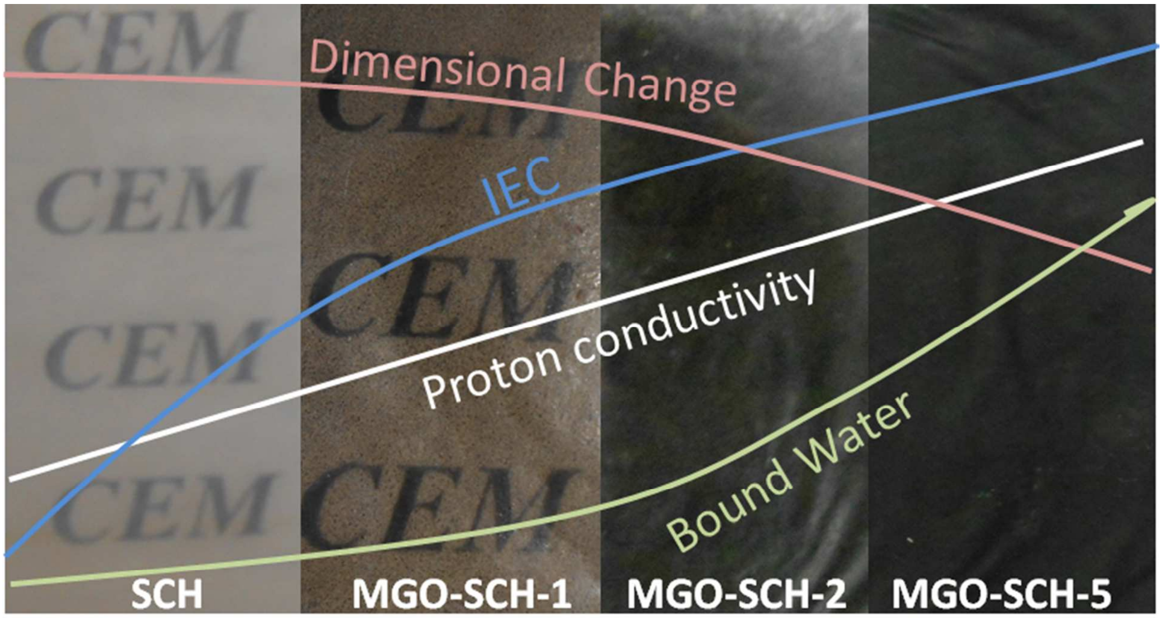
CEM
Dimensional Change
IEC
Proton conductivity
Bound Water
SCH
MGO-SCH-1
MGO-SCH-2
MGO-SCH-5